Original Article | Gastrointestinal Imaging

eISSN 2005-8330
https://doi.org/10.3348/kjr.2021.0134
Korean J Radiol 2022;23(1):42-51

Korean Journal of Radiology
KJR

Direction of Tissue Contraction after Microwave Ablation: A Comparative Experimental Study in *Ex Vivo* Bovine Liver

Junhyok Lee[1], Hyunchul Rhim[1, 2], Min Woo Lee[2, 3], Tae Wook Kang[2], Kyoung Doo Song[2], Jeong Kyong Lee[4]

Departments of [1]Medical Device Management and Research and [3]Health Sciences and Technology, SAIHST, Sungkyunkwan University, Seoul, Korea; [2]Department of Radiology and Center for Imaging Science, Samsung Medical Center, Sungkyunkwan University School of Medicine, Seoul, Korea; [4]Department of Radiology, Mokdong Hospital, Ewha Womans University, School of Medicine, Seoul, Korea

Objective: This study aimed to investigate the direction of tissue contraction after microwave ablation in *ex vivo* bovine liver models.

Materials and Methods: Ablation procedures were conducted in a total of 90 sites in *ex vivo* bovine liver models, including the surface (n = 60) and parenchyma (n = 30), to examine the direction of contraction of the tissue in the peripheral and central regions from the microwave antenna. Three commercially available 2.45-GHz microwave systems (Emprint, Neuwave, and Surblate) were used. For surface ablation, the lengths of two overlapped square markers were measured after 2.5- and 5-minutes ablations (n = 10 ablations for each system for each ablation time). For parenchyma ablation, seven predetermined distances between the markers were measured on the cutting plane after 5- and 10-minutes ablations (n = 5 ablations for each system for each ablation time). The contraction in the radial and longitudinal directions and the sphericity index (SI) of the ablation zones were compared between the three systems using analysis of variance.

Results: In the surface ablation experiment, the mean longitudinal contraction ratio and SI from a 5-minutes ablation using the Emprint, Neuwave, and Surblate systems were 28.92% and 1.04, 20.10% and 0.53, and 24.90% and 0.45, respectively ($p < 0.001$). A positive correlation between longitudinal contraction and SI was noted, and a similar radial contraction was observed. In the parenchyma ablation experiment, the mean longitudinal contraction ratio and SI from a 10-minutes ablation using the three pieces of equipment were 38.60% and 1.06, 32.45% and 0.61, and 28.50% and 0.50, respectively ($p < 0.001$). There was a significant difference in the longitudinal contraction properties, whereas there was no significant difference in the radial contraction properties.

Conclusion: The degree of longitudinal contraction showed significant differences depending on the microwave ablation equipment, which may affect the SI of the ablation zone.

Keywords: *Microwave; Thermal ablation; Tissue contraction; Ablation zone shape; Sphericity index*

INTRODUCTION

Tissue contraction is clinically significant, particularly for image-guided thermal therapies, such as microwave ablation (MWA). Any changes in tissue dimensions should be considered when planning and assessing treatment [1]. At high temperatures, tissue contraction is positively correlated with local tissue dehydration, protein denaturation, and collagen contraction [2]. Accordingly, the post-treatment ablation zone may underestimate the extent of the original tissue included within the coagulation zone [3].

Many recent studies have described tissue contraction

Received: May 3, 2020 **Revised:** July 11, 2021 **Accepted:** August 16, 2021
Corresponding author: Hyunchul Rhim, MD, PhD, Department of Radiology and Center for Imaging Science, Samsung Medical Center, Sungkyunkwan University School of Medicine, 81 Irwon-ro, Gangnam-gu, Seoul 06351, Korea.
• E-mail: rhim.hc@gmail.com

Korean Journal of Radiology
KJR

during thermal ablation [2-9]. Such a phenomenon may affect the assessment of the therapeutic efficacy and safety of unwanted heating of any abutting vital structures [5]. Therefore, the phenomenon of tissue contraction should be considered for accurate predictions and assessments of ablation outcomes [10]. Farina et al. [9] reported that a substantial asymmetric contraction of the ablated tissue volume as well as an initial expansion phenomenon occurs during MWA. Subsequently, they evaluated the extent of tissue contraction using three commercial MWA devices [5]. In the radial direction, similar trends in contraction were observed at the margin of the thermally ablated areas, whereas in the longitudinal direction, one device induced different contraction kinetics with respect to the other two [5]. However, in the experimental setup, the relatively small cubes of *ex vivo* liver in a variety of sizes embedded in the agar phantom restricted the measurements of the ablation dimensions.

Liu et al. [4] evaluated tissue contraction by measuring the displacement of a fiducial marker using computed tomography imaging during the ablation of the *ex vivo* liver. They discovered that the strength of contraction in the radial direction transverse to the antenna was relatively stronger than that in the longitudinal direction of the antennal axis. Thus, ablations appeared to be more elongated than the initial tissue because of the strong trend of contraction in the transverse plane.

The abovementioned studies [4,5,9] focused on tissue contraction in the radial direction from the antennal axis and reported a trend of relatively low contraction in the longitudinal direction. Most MWA devices appear to inflict an ellipsoidal ablation with low predictability with respect to size [11-13]. Recently, a new MWA device that can create a more spherical ablation zone was introduced in the clinical setting [14,15]. However, the mechanism underlying MWA has not been clearly evaluated based on the properties of tissue contraction.

This study aimed to objectively assess tissue contraction in the radial and longitudinal directions associated with MWA using three different systems in *ex vivo* bovine liver models and to elucidate the correlation between tissue contraction and sphericity of the ablation zone across the systems.

MATERIALS AND METHODS

MWA Equipment

Commercial MWA apparatuses operating at 2.45 GHz, the Emprint™ (Medtronic) with a 13G water-cooled antenna, NEUWAVE™ (J&J Medical Devices) with a CO_2-cooled 17G PR probe, and SurBlate™ (Vison Medical USA) with a 15G water-cooled antenna were used for this experimental study. In all experiments, the microwave power was set according to the manufacturer's recommendations, namely 100 W for the Emprint, 65 W for the NEUWAVE, and 100 W for the SurBlate.

Preparation of Tissue Samples

Freshly excised normal bovine livers weighing an average of 7 kg each were obtained from a local slaughterhouse (Hyupjin Center) on the day of each experiment and were cut into rectangular blocks (13 x 11 x 8 cm [length x width x height]) at room temperature.

Two *ex vivo* Bovine Experimental Models

Weiss et al. [16] analyzed the planar strain of *ex vivo* liver during MWA and postulated that rapid enlargement within approximately 3 minutes occurs due to the thermal expansion of tissue surrounding the antenna, combined with an increase in the vapor pressure of its fluids. Once denaturation of the proteins and desiccation start to occur, the tissue begins to contract. This result led us to assign ablation times of 2.5 and 5 minutes for surface contraction and 5 and 10 minutes for parenchyma contraction because the contraction was assumed to occur after approximately 3 minutes of ablation. To observe the contraction of the central and peripheral regions from the antenna, the parenchyma and surface ablation experiments were conducted with the same 5-minutes ablation time.

Surface Ablation

The surface of the liver was pigmented with two overlapped squares of size 1.95 x 1.95 cm and 2.95 x 2.95 cm, respectively, using a grid frame and SEPIA MicroPigment (The Standard), which is an endoscopic marker used for polyps and lesions in the gastrointestinal tract. Then, an antenna was placed at the center of the square marker, so that the end of the antennal tip was located at the bottom of the square (Fig. 1). Given that the ablation diameter in the *ex vivo* experiment was approximately 2–5 cm, depending on each device [12], the square size was assigned to be similar to the ablation diameter. Using each MWA device, two different ablation times of 2.5 and 5 minutes were applied, and 10 ablation zones were investigated at each ablation time.

 https://doi.org/10.3348/kjr.2021.0134

The lengths of the eight sides of the two overlapped square markers were measured (Fig. 1), and a total of 160 data points were acquired from each device. The lengths of the top and bottom sides of the two squares were assigned as the contraction in the radial direction orthogonal to the antennal axis, whereas the lengths of the left and right sides of the two squares were assigned as the contraction in the longitudinal direction parallel to the antennal axis. The contraction ratio was estimated from the mean value of the contraction length in the radial and longitudinal directions. The ablation zone size was also estimated by measuring the radial axis diameter (RAD) perpendicular to the antennal axis and the longitudinal axis diameter (LAD) along the antennal axis using ImageJ 1.42 (http://rsbweb.nih.gov/ij/download.html). The sphericity index (SI) of the ablation zones was calculated using the following formula: $SI = RAD^2/LAD^2$ (Fig. 2).

Parenchyma Ablation

The parenchyma of the liver was internally pigmented with ten markers using a specially designed fixture with ten needles (19G), each with a sheath (18G). The intervals

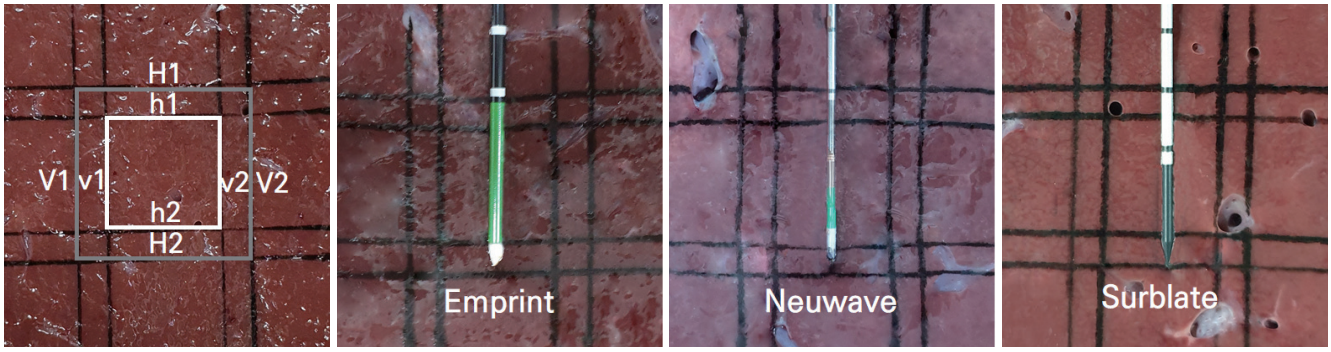

Fig. 1. Schema of surface ablation. The outer square (gray/2.95 x 2.95 cm) and inner square (white/1.95 x 1.95 cm) markers were overlapped on the surface of the liver. The left and right sides of the squares are the indices of contraction in the longitudinal direction parallel to the antennal axis, whereas the top and bottom sides of the squares are the indices of contraction in the radial direction orthogonal to the antennal axis. H1 and H2 = index of contraction in the radial direction in the outer square (gray), h1 and h2 = index of contraction in the radial direction in the inner square (white), V1 and V2 = index of contraction in the longitudinal direction in the outer square (gray), v1 and v2 = index of contraction in the longitudinal direction in the inner square (white).

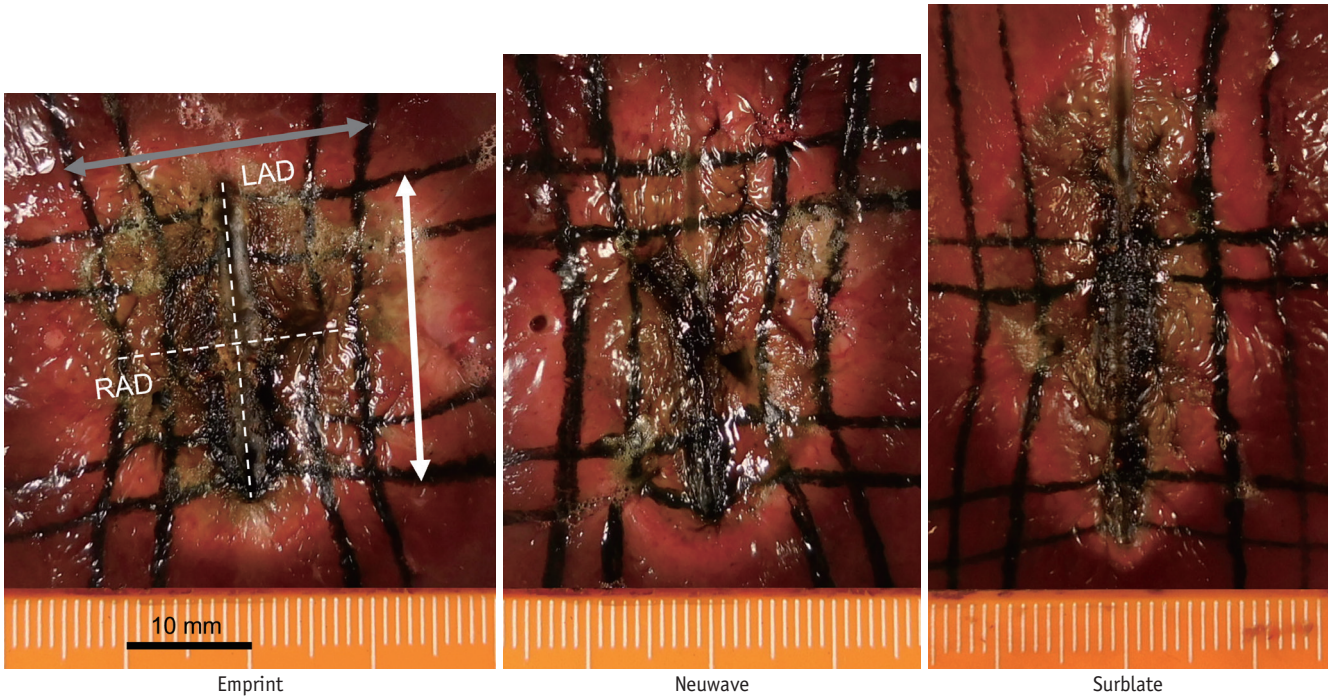

Fig. 2. Images after a 5-minutes ablation on the surface of the bovine liver. The shape of the ablation zone and tissue contraction can be seen in both the radial (gray) and longitudinal (white) directions. LAD = longitudinal axis diameter, RAD = radial axis diameter

https://doi.org/10.3348/kjr.2021.0134

Korean Journal of Radiology
KJR

between the pigmented markers were as follows: H1, 1 cm; H2, 1 cm; H3, 1 cm; H4, 2 cm; H5, 3 cm; V1, 2 cm; and V2, 2 cm (Fig. 3). After puncturing the liver directly with the ten needles, the ten sheaths were left behind by pulling out only the needles, after which ten rods (21G) dipped into the MicroPigment were placed into each sheath. The ten sheaths were then pulled out, while the ten dyed rods were left behind. Finally, an antenna was inserted into the liver, and the ten rods were pulled down. From each MWA equipment, two different ablation times of 5 and 10 minutes were used, and five ablation zones were investigated at each ablation time.

The lengths of the seven intervals from the ten pigmented markers on the cutting plane along the antennal axis were measured (Fig. 4), and 70 data points were acquired for each MWA device. The interval length from H1 to H5 was assigned as the contraction in the radial direction orthogonal to the antennal axis, whereas the interval lengths of V1 and V2 were assigned as the contraction in the longitudinal direction parallel to the antennal axis. The contraction ratio was estimated from the mean value of the contraction length in the radial and longitudinal directions. The ablation zone size (RAD, LAD) was estimated, and the SI was calculated. The ablation volume was estimated using the formula for an ellipsoid: $V = (\pi/6) \times RAD^2 \times LAD$.

Statistical Analysis

Differences in the length of tissue contraction between the three pieces of equipment were analyzed using one-way analysis of variance (R ver. 3.4.4 with RStudio ver. 1.1.442). The Shapiro–Wilk test for normality checks and Bartlett's test for homogeneity of variances were performed, and the assumptions were met. Post hoc comparisons using Tukey's honestly significant difference (HSD) test were performed. Statistical significance was set at $p < 0.05$.

RESULTS

Surface Ablation

For liver surface ablation using each piece of equipment, the tissue contraction ratios with respect to the directions and SI are shown in Table 1. Remarkably, the ablation shape of the Surblate extended out of the marker area along the antennal axis (Fig. 2), which caused inaccurate

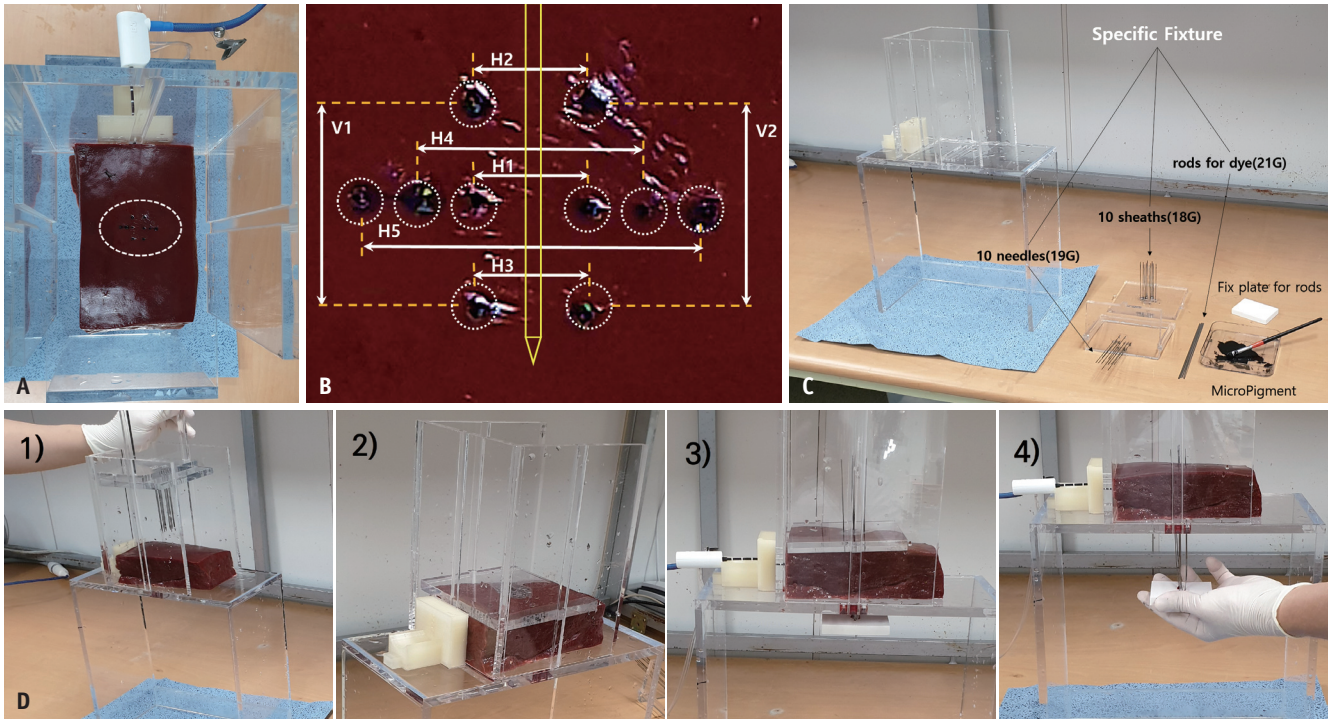

Fig. 3. Schema of parenchyma ablation.
A. Inserted antenna after dipping into the pigmented markers. **B.** Magnified image of the dotted circle from **(A)** and the antennal position. The interval lengths of H1, H2, H3, H4, H5, V1, V2 are 1, 1, 1, 2, 3, 2, and 2 cm, respectively. **C.** Specific fixture in which dot markers and tools, such as the biopsy needle comprising a needle, sheath, and rod for pigmenting were used. **D.** 1) puncturing by assembling the sheath and needle fixture, 2) moving out the needle fixture, 3) inserting the dyed rods inside the sheaths after inserting the antenna, 4) pulling down the dyed rods to pigment the marker.

https://doi.org/10.3348/kjr.2021.0134

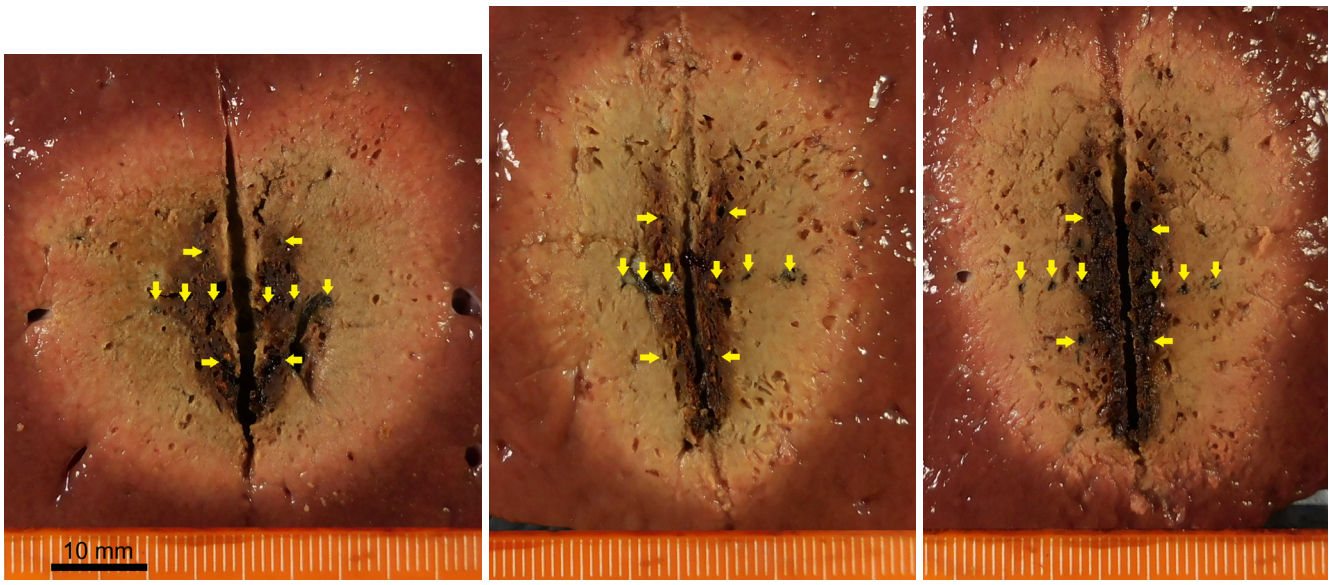

Fig. 4. Images after a 10-minutes ablation in the parenchyma of the bovine liver. Ten pigmented markers indicated with yellow arrows are displayed on the cut section.

measurements of the contraction. For the 5-minutes ablation and inner square condition, the mean longitudinal contraction ratio and SI were 28.92% and 1.04, respectively, for the Emprint system, and 20.10% and 0.53, respectively, for the Neuwave system. The Emprint and Neuwave systems showed similar trends in that the SI was correlated with the contraction ratio in the longitudinal direction. The Emprint and Neuwave systems revealed a similarity in contraction in the radial direction and indicated that a low SI is expected when the discrepancy between the contraction in the radial direction and contraction in the longitudinal direction was high. In the 2.5-minutes ablation experiment, no thermal expansion-related phenomena were observed.

Parenchyma Ablation

For parenchymal ablation of the liver with each MWA system, the tissue contraction ratio according to the direction and SI are shown in Table 2. Because the interval length from H1 to H5, regarded as the contraction in the radial direction, was not significantly different in the analysis of each system, the same intervals H1, H2, and H3 were selected to investigate the contraction in the radial direction. In the 10-minutes ablation condition, the mean longitudinal contraction ratio and SI of the three systems were 38.60% and 1.06, 32.45% and 0.61, and 28.50% and 0.50 for the Emprint, Neuwave, and Surblate, respectively. A similar radial contraction was observed, and a low SI was expected when the discrepancy between the radial and longitudinal contraction ratios was high (Fig. 5). There was a significant difference in longitudinal contraction (p < 0.001), whereas there was no significant difference in radial contraction.

A trend in contraction with respect to direction in each of the three devices was observed (Fig. 6). The contraction levels in both directions increased with time. Contraction in the radial direction converged at a similar level over time. However, contraction in the longitudinal direction was sustained at different levels with each device. According to the 5-minutes ablation experimental contraction data, a difference in longitudinal contraction between the surface and parenchyma was observed, which indicated a trend of high contraction in the central region from the antenna.

The estimated mean ablation volumes for each device were 96.15 cm^3 (Emprint), 71.29 cm^3 (Neuwave), and 66.18 cm^3 (Surblate).

DISCUSSION

Ablation is widely considered to be a safe and curative procedure. The use of MWA has increased in popularity owing to its better ablation performance at high temperatures and shorter ablation times [17]. However, a more refined ablation strategy is required to optimally ablate the index tumor, especially in patients with poor liver function. In that sense, a clear understanding of the ablation zone profile, including tissue contraction, is

https://doi.org/10.3348/kjr.2021.0134

Korean Journal of Radiology
KJR

Table 1. Comparison of Contraction and the SI between Surface Ablations

	Emprint (n = 10)	Neuwave (n = 10)	Surblate (n = 10)	*P**
2.5 minutes ablation time				
Radial tissue contraction				
Inner square-length, cm	1.42 ± 0.13	1.40 ± 0.12	1.54 ± 0.16	0.004[‡§]
Inner square-contraction ratio, %	27.18 ± 6.55	28.26 ± 6.22	21.13 ± 8.16	
Outer square-length, cm	2.59 ± 0.17	2.59 ± 0.15	2.64 ± 0.20	0.643
Outer square-contraction ratio, %	12.12 ± 5.58	12.20 ± 5.14	10.66 ± 6.64	
Longitudinal tissue contraction				
Inner square-length, cm	1.56 ± 0.09	1.58 ± 0.13	1.65 ± 0.08	0.004[§]
Inner square-contraction ratio, %	19.95 ± 4.66	19.10 ± 6.89	15.36 ± 3.89	
Outer square-length, cm	2.64 ± 0.12	2.66 ± 0.12	2.61 ± 0.10	0.370
Outer square-contraction ratio, %	10.39 ± 3.98	9.96 ± 4.16	11.41 ± 3.29	
Ablation zone				
RAD, cm	2.81 ± 0.14	2.21 ± 0.10	2.04 ± 0.15	< 0.001[†‡§]
LAD, cm	2.80 ± 0.10	3.06 ± 0.15	3.48 ± 0.19	< 0.001[†‡§]
SI	1.01 ± 0.12	0.52 ± 0.06	0.34 ± 0.07	< 0.001[†‡§]
5 minutes ablation time				
Radial tissue contraction				
Inner square-length, cm	1.24 ± 0.12	1.28 ± 0.09	1.41 ± 0.19	0.007[‡§]
Inner square-contraction ratio, %	36.36 ± 6.11	34.56 ± 4.51	27.64 ± 9.79	
Outer square-length, cm	2.30 ± 0.22	2.37 ± 0.14	2.43 ± 0.25	0.136
Outer square-contraction ratio, %	22.08 ± 7.60	19.53 ± 4.88	17.53 ± 8.39	
Longitudinal tissue contraction				
Inner square-length, cm	1.39 ± 0.15	1.56 ± 0.14	1.47 ± 0.13	0.001[†]
Inner square-contraction ratio, %	28.92 ± 7.54	20.10 ± 7.27	24.90 ± 6.52	
Outer square-length, cm	2.35 ± 0.19	2.55 ± 0.20	2.34 ± 0.15	< 0.001[†‡]
Outer square-contraction ratio, %	20.24 ± 6.35	13.42 ± 6.68	20.58 ± 5.03	
Ablation zone				
RAD, cm	3.41 ± 0.20	2.72 ± 0.12	2.63 ± 0.15	< 0.001[†‡§]
LAD, cm	3.35 ± 0.17	3.73 ± 0.12	3.92 ± 0.17	< 0.001[†‡§]
SI	1.04 ± 0.09	0.53 ± 0.07	0.45 ± 0.04	< 0.001[†‡§]

Radial tissue contraction inner square-length (h1, h2; 1.95 cm). Radial tissue contraction Outer square-Length (H1, H2; 2.95 cm). Longitudinal tissue contraction inner square-length (v1, v2; 1.95 cm). Longitudinal tissue contraction Outer square-Length (V1, V2; 2.95 cm). Data are mean ± standard deviation. *One-way analysis of variance test (differences statistically not significant if $p > 0.05$), [†‡§]Indicate significant pairwise comparisons according to the Tukey's HSD post hoc test: [†]Emprint vs. Neuwave, [‡]Neuwave vs. Surblate, [§]Surblate vs. Emprint. LAD = longitudinal axis diameter, RAD = radial axis diameter, SI = sphericity index

essential to achieve better outcomes with MWA.

The current experimental study demonstrated that the direction of tissue contraction varies depending on the commercial microwave equipment used, especially along the longitudinal axis. Although many previous studies have proven that radial contraction (shrinkage) is more prominent than longitudinal contraction, no study has demonstrated that the direction of contraction depends on the type of microwave equipment. The results of the present study show that the difference in the degree of contraction between the radial and longitudinal directions can affect the spherical index of the ablation zone. We can predict the real ablation zone and volume based on this difference in the contraction profile depending on the microwave equipment. This will be critical for achieving an optimal ablation volume with adequate ablation margins and avoiding unwanted thermal injury to adjacent vital organs [18,19].

In this study, we examined tissue contraction in the radial and longitudinal directions, and identified the characteristics of the ablation zone shape for each MWA device. The results showed that longitudinal contractions were different, whereas radial contractions were similar across the MWA devices. The spherical ablation zone shape had an almost equivalent tissue contraction ratio in both the radial and longitudinal directions. Each MWA device produced substantially different ablation volumes

 https://doi.org/10.3348/kjr.2021.0134

Table 2. Comparison of Contraction and the SI between Parenchyma Ablations

	Emprint (n = 5)	Neuwave (n = 5)	Surblate (n = 5)	*P**
5 minutes ablation time				
Radial tissue contraction				
Length, cm	0.68 ± 0.09	0.68 ± 0.09	0.67 ± 0.08	0.924
Contraction ratio, %	32.13 ± 8.64	32.26 ± 8.88	33.27 ± 7.98	
Longitudinal tissue contraction				
Length, cm	1.22 ± 0.13	1.40 ± 0.11	1.51 ± 0.18	< 0.001†§
Contraction ratio, %	39.20 ± 6.63	30.05 ± 5.37	24.5 ± 8.99	
Ablation zone				
RAD, cm	3.11 ± 0.04	2.69 ± 0.16	2.71 ± 0.16	< 0.001†§
LAD, cm	3.15 ± 0.08	3.81 ± 0.18	4.32 ± 0.37	< 0.001†‡§
SI	0.97 ± 0.04	0.50 ± 0.07	0.39 ± 0.04	< 0.001†‡§
10 minutes ablation time				
Radial tissue contraction				
Length, cm	0.64 ± 0.09	0.65 ± 0.07	0.66 ± 0.11	0.828
Contraction ratio, %	36.40 ± 8.80	34.87 ± 7.41	34.40 ± 11.29	
Longitudinal tissue contraction				
Length, cm	1.23 ± 0.05	1.35 ± 0.11	1.43 ± 0.09	< 0.001†§
Contraction ratio, %	38.60 ± 2.69	32.45 ± 5.61	28.50 ± 4.65	
Ablation zone				
RAD, cm	4.18 ± 0.15	3.51 ± 0.08	3.38 ± 0.11	< 0.001†§
LAD, cm	4.06 ± 0.15	4.51 ± 0.19	4.78 ± 0.17	< 0.001†§
SI	1.06 ± 0.10	0.61 ± 0.06	0.50 ± 0.06	< 0.001†§

Radial tissue contraction Length (H1, H2, H3; 1 cm). Longitudinal tissue contraction Length (V1, V2; 2 cm). Data are mean ± standard deviation. *One-way analysis of variance test (differences statistically not significant if $p > 0.05$), †‡§Indicate significant pairwise comparisons according to the Tukey's HSD post hoc test: †Emprint vs. Neuwave, ‡Neuwave vs. Surblate, §Surblate vs. Emprint. LAD = longitudinal axis diameter, RAD = radial axis diameter, SI = sphericity index

and shapes because each SI value was different and time independent.

The Emprint system has unique properties allowing it to reliably produce a spherical ablation zone of a particular shape by field and wavelength control [14]. The clinical performance of these controls has been compared with that of two other routinely used conventional MWA systems, revealing that a more spherical ablation zone and a larger minimal ablative margin can be obtained with field and wavelength control [15]. Furthermore, the antenna is a critical component that transfers microwave energy into the tissue to form an active heating zone [20], and its design is important for supplying efficient radiation into the surrounding tissue to maximize energy delivery and to control the radiation pattern to obtain the desired ablation zone geometry [11,21-24].

Several studies have evaluated tissue contraction in other models. Brace et al. [2] described tissue contraction in liver and lung tissue resulting from microwave and radiofrequency (RF) ablation, which can heat tissue to 100°C or more, noting an approximately 25% reduction in ablation zone diameter. Sommer et al. [3] described a similar tissue shrinkage and dehydration caused by MWA, noting an approximately 30% underestimation of effective coagulation in the kidneys. Rossmann et al. [7] developed another model based on studies of tissue shrinkage during controlled temperature exposure from 60°C to 95°C, and suggested 12.3%–21.7% shrinkage after 15 minutes of temperature exposure. Liu and Brace [4,8] described tissue contraction spatially through fiducial marker movement using CT imaging during MWA. From the localized displacement of markers, central tissue contracted by more than 60% and peripheral tissue contracted by only 15% in any direction. The authors simulated temperature-dependent contraction using numerical modeling. While these studies lacked analysis of longitudinal contraction and relied on comparing independent samples, the contraction rate of the present study is similar to that of previous studies and has been verified through comparative studies.

Farina et al. [9] and Weiss et al. [16] reported that thermal expansion was due to the presence of liquid vaporization at high temperatures. Both studies used a

https://doi.org/10.3348/kjr.2021.0134

Korean Journal of Radiology
KJR

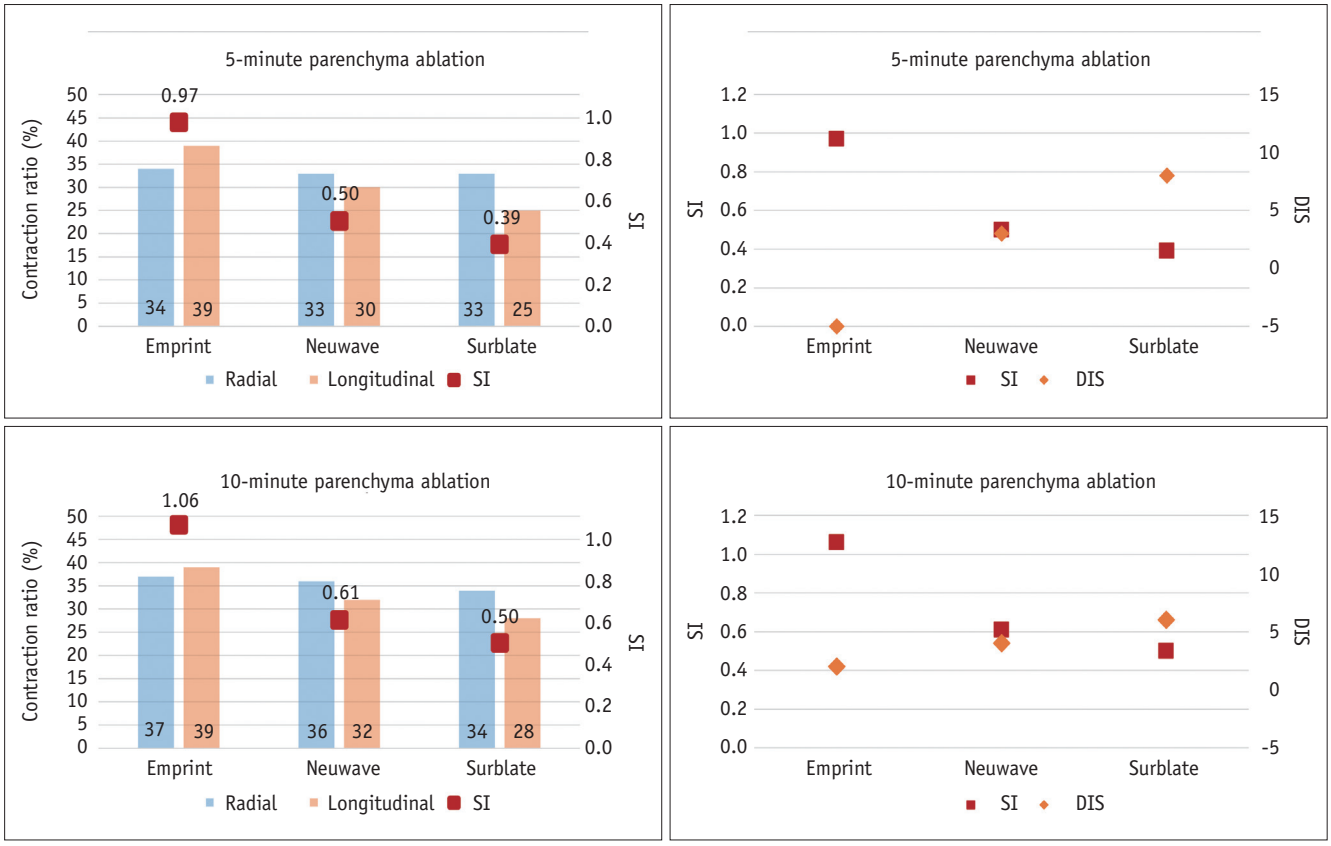

Fig. 5. The Radial and Longitudinal compared with the SI. The sphericity of each device was sustained in a similar manner, although the ablation time increased. The DIS of the three microwave ablation systems was inversely proportional to the sphericity. DIS = discrepancy between radial and longitudinal contraction ratio, Longitudinal = contraction ratio in the longitudinal direction, Radial = contraction ratio in the radial direction, SI = sphericity index

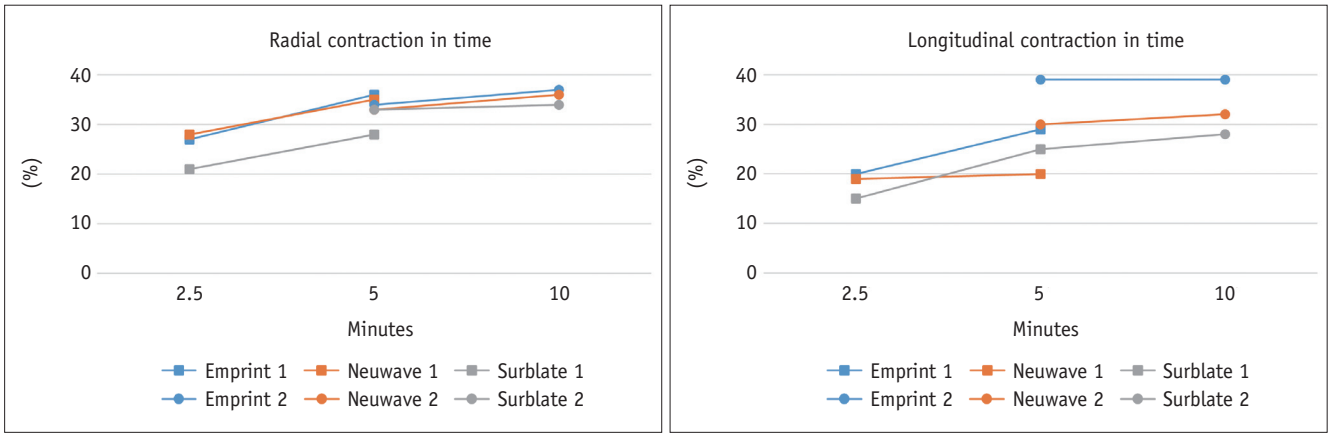

Fig. 6. The contraction trend with respect to direction in each device. The contraction levels in both directions increased with time. The Radial converged at a similar level with increasing time. The Longitudinal was sustained at different levels in each device. Longitudinal = contraction ratio in the longitudinal direction, Radial = contraction ratio in the radial direction, 1 = inner square/surface ablation (square mark), 2 = parenchyma ablation (circle mark)

container in which the bovine liver was placed to assess the expansion phenomenon. In contrast, surface ablation experiments were conducted in open chambers unsuitable for observing the expansion phenomenon. It was speculated that the evaporation pressure naturally dissipated owing to the surface experimental conditions.

This study had several limitations. First, the current results were only based on *ex vivo* experimental studies,

 https://doi.org/10.3348/kjr.2021.0134

and should be demonstrated by *in vivo* and clinical studies. However, there are many technical hurdles to objectively measure tissue contraction using any marker in living animals or humans. Second, a more detailed assessment of tissue contraction in a wider area of the liver was not available because of technical difficulties with regard to the extensive placement of pigmented markers and limited experimental resources. The lack of markers that did not cover the entire ablation zone limited the detailed analysis of contraction in the ablation zone; in particular, the square grid marker in the surface ablation experiment did not cover the entire ablation zone in the data of one of the MWA systems. Therefore, we did not achieve statistically significant results in this study. Finally, further investigation using variable ablation parameters beyond the manufacturer's recommendation is warranted to fully explore the characteristics of tissue contraction following MWA and to compare them with RF devices.

In conclusion, the degree of tissue contraction did not differ along the radial direction, and it varied along the longitudinal direction depending on the microwave equipment used in our *ex vivo* experimental model. A similar contraction profile in both directions may help create a more spherical ablation zone, which is ideal for the optimal configuration of the ablation zones and circumferential ablative margins.

Availability of Data and Material

The datasets generated or analyzed during the study are available from the corresponding author on reasonable request.

Conflicts of Interest

Min Woo Lee who is on the editorial board of the *Korean Journal of Radiology* was not involved in the editorial evaluation or decision to publish this article. All remaining authors have declared no conflicts of interest.

Acknowledgments

We thank Dong Un Kim, B.S. (Korea) for his technical assistance in the *ex-vivo* experiment.

Author Contributions

Conceptualization: Hyunchul Rhim, Min Woo Lee, Tae Wook Kang, Kyoung Doo Song, Jeong Kyong Lee. Data curation: Junhyok Lee. Formal analysis: Junhyok Lee. Investigation: Junhyok Lee. Methodology: Hyunchul Rhim, Min Woo Lee, Tae Wook Kang, Kyoung Doo Song, Jeong Kyong Lee. Project administration: Hyunchul Rhim. Resources: Junhyok Lee. Software: Junhyok Lee. Supervision: Hyunchul Rhim. Validation: Junhyok Lee. Visualization: Junhyok Lee. Writing—original draft: Junhyok Lee. Writing—review & editing: Hyunchul Rhim.

ORCID iDs

Junhyok Lee
https://orcid.org/0000-0002-3276-8845
Hyunchul Rhim
https://orcid.org/0000-0002-9737-0248
Min Woo Lee
https://orcid.org/0000-0001-9048-9011
Tae Wook Kang
https://orcid.org/0000-0002-0725-8317
Kyoung Doo Song
https://orcid.org/0000-0002-2767-3622
Jeong Kyong Lee
https://orcid.org/0000-0002-5507-0140

Funding Statement

None

REFERENCES

1. Lee JK, Siripongsakun S, Bahrami S, Raman SS, Sayre J, Lu DS. Microwave ablation of liver tumors: degree of tissue contraction as compared to RF ablation. *Abdom Radiol (NY)* 2016;41:659-666
2. Brace CL, Diaz TA, Hinshaw JL, Lee FT Jr. Tissue contraction caused by radiofrequency and microwave ablation: a laboratory study in liver and lung. *J Vasc Interv Radiol* 2010;21:1280-1286
3. Sommer CM, Sommer SA, Mokry T, Gockner T, Gnutzmann D, Bellemann N, et al. Quantification of tissue shrinkage and dehydration caused by microwave ablation: experimental study in kidneys for the estimation of effective coagulation volume. *J Vasc Interv Radiol* 2013;24:1241-1248
4. Liu D, Brace CL. Evaluation of tissue deformation during radiofrequency and microwave ablation procedures: influence of output energy delivery. *Med Phys* 2019;46:4127-4134
5. Farina L, Nissenbaum Y, Cavagnaro M, Goldberg SN. Tissue shrinkage in microwave thermal ablation: comparison of three commercial devices. *Int J Hyperthermia* 2018;34:382-391
6. Amabile C, Farina L, Lopresto V, Pinto R, Cassarino S, Tosoratti N, et al. Tissue shrinkage in microwave ablation of liver: an ex vivo predictive model. *Int J Hyperthermia* 2017;33:101-109
7. Rossmann C, Garrett-Mayer E, Rattay F, Haemmerich D. Dynamics of tissue shrinkage during ablative temperature

exposures. *Physiol Meas* 2014;35:55-67
8. Liu D, Brace CL. CT imaging during microwave ablation: analysis of spatial and temporal tissue contraction. *Med Phys* 2014;41:113303
9. Farina L, Weiss N, Nissenbaum Y, Cavagnaro M, Lopresto V, Pinto R, et al. Characterisation of tissue shrinkage during microwave thermal ablation. *Int J Hyperthermia* 2014;30:419-428
10. Kim C. Understanding the nuances of microwave ablation for more accurate post-treatment assessment. *Future Oncol* 2018;14:1755-1764
11. Lubner MG, Brace CL, Hinshaw JL, Lee FT Jr. Microwave tumor ablation: mechanism of action, clinical results, and devices. *J Vasc Interv Radiol* 2010;21:S192-S203
12. Ruiter SJS, Heerink WJ, de Jong KP. Liver microwave ablation: a systematic review of various FDA-approved systems. *Eur Radiol* 2019;29:4026-4035
13. Fallahi H, Prakash P. Antenna designs for microwave tissue ablation. *Crit Rev Biomed Eng* 2018;46:495-521
14. Alonzo M, Bos A, Bennett S, Ferral H. The emprint™ ablation system with thermosphere™ technology: one of the newer next-generation microwave ablation technologies. *Semin Intervent Radiol* 2015;32:335-338
15. Vogl TJ, Basten LM, Nour-Eldin NA, Kaltenbach B, Bodelle B, Wichmann JL, et al. Evaluation of microwave ablation of liver malignancy with enabled constant spatial energy control to achieve a predictable spherical ablation zone. *Int J Hyperthermia* 2018;34:492-500
16. Weiss N, Goldberg SN, Nissenbaum Y, Sosna J, Azhari H. Planar strain analysis of liver undergoing microwave thermal ablation using x-ray CT. *Med Phys* 2015;42:372-380
17. Lencioni R, de Baere T, Martin RC, Nutting CW, Narayanan G. Image-guided ablation of malignant liver tumors: recommendations for clinical validation of novel thermal and non-thermal technologies-a western perspective. *Liver Cancer* 2015;4:208-214
18. Park MJ, Kim YS, Rhim H, Lim HK, Lee MW, Choi D. A comparison of US-guided percutaneous radiofrequency ablation of medium-sized hepatocellular carcinoma with a cluster electrode or a single electrode with a multiple overlapping ablation technique. *J Vasc Interv Radiol* 2011;22:771-779
19. Ierardi AM, Mangano A, Floridi C, Dionigi G, Biondi A, Duka E, et al. A new system of microwave ablation at 2450 MHz: preliminary experience. *Updates Surg* 2015;67:39-45
20. Hinshaw JL, Lubner MG, Ziemlewicz TJ, Lee FT Jr, Brace CL. Percutaneous tumor ablation tools: microwave, radiofrequency, or cryoablation--what should you use and why? *Radiographics* 2014;34:1344-1362
21. Brace CL. Microwave ablation technology: what every user should know. *Curr Probl Diagn Radiol* 2009;38:61-67
22. Brace CL. Radiofrequency and microwave ablation of the liver, lung, kidney, and bone: what are the differences? *Curr Probl Diagn Radiol* 2009;38:135-143
23. Brace CL. Microwave tissue ablation: biophysics, technology, and applications. *Crit Rev Biomed Eng* 2010;38:65-78
24. Brace C. Thermal tumor ablation in clinical use. *IEEE Pulse* 2011;2:28-38

 https://doi.org/10.3348/kjr.2021.0134